

Electronic Supplementary Information:

Symmetry-breaking charge separation in weakly coupled anthracene dimers

Liping Lv^{†, a}, Heyuan Liu^{†, a, *}, Tianyu Li^a, Boce Cui^a, Tianying Wang^a, Xiaojuan Song^a,
Wenmiao Chen^b, Yanli Chen^a, and Xiyou Li^{a, *}

Content

1. ¹ H NMR spectra and MALDI-TOF spectra of Ph-BPEA and <i>o-/m-/p-</i> dimer 2	
2. CV and DPV of Ph-BPEA and <i>o-/m-/p-</i> dimer	6
3. Solvent-polarity-dependent absorption experiment of <i>o-/m-/p-</i> dimer	7
4. The fluorescence spectra and dynamics of monomer Ph-BPEA	8
5. <i>fs</i> -TA spectra of <i>o-/m-/p-</i> dimer in THF excited at 420 nm	9
6. Electron transfer experiment	11
7. <i>fs</i> -TA spectra of <i>o-/m-/p-</i> dimer in polystyrene (PS) film and polymethyl methacrylate (PMMA) film	12
8. Charge separation and charge recombination rates	13
9. Theoretical calculation	19

1. ^1H NMR spectra and MALDI-TOF spectra of Ph-BPEA and *o*-/*m*-/*p*- dimer

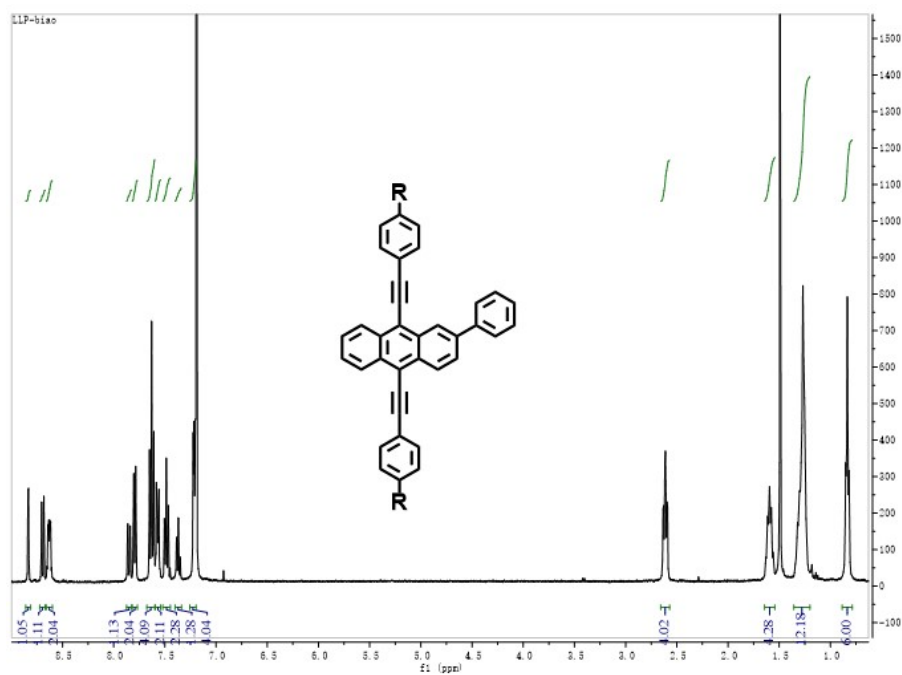


Fig. S1 The ^1H NMR spectrum of Ph-BPEA.

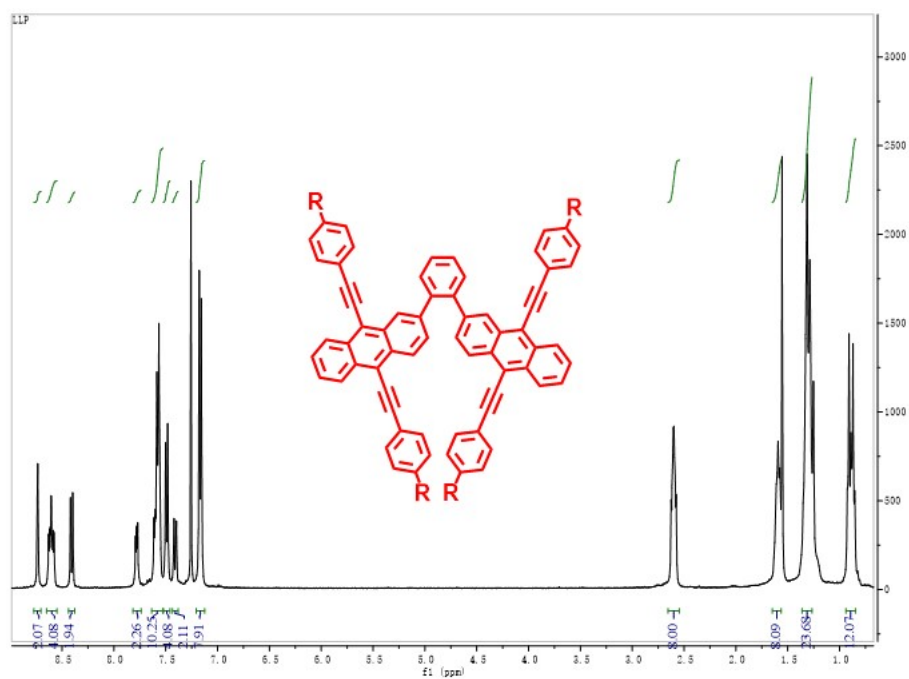


Fig. S2 The ^1H NMR spectrum of *o*-dimer.

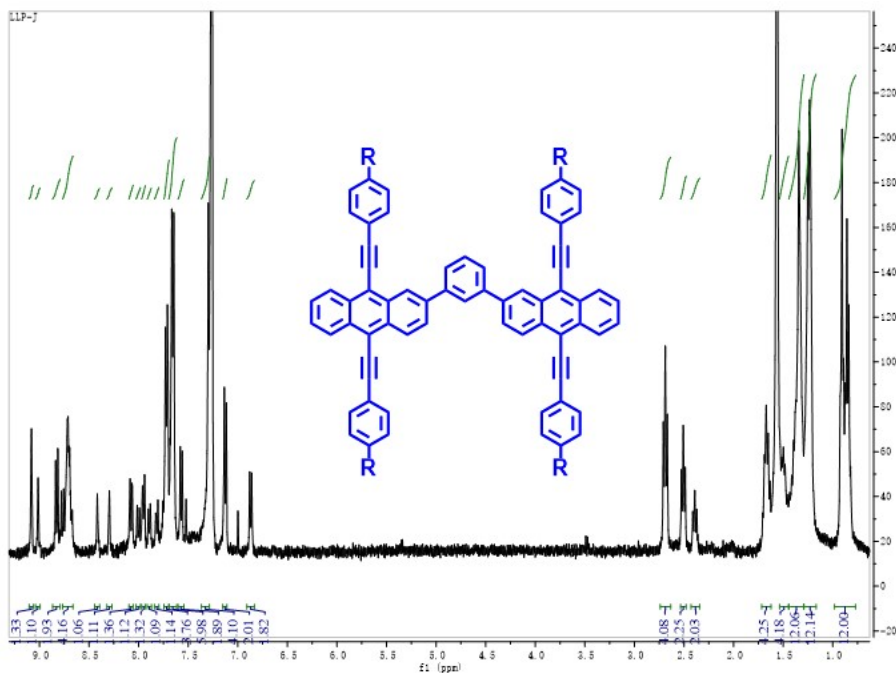


Fig. S3 The ^1H NMR spectrum of *m*-dimer.

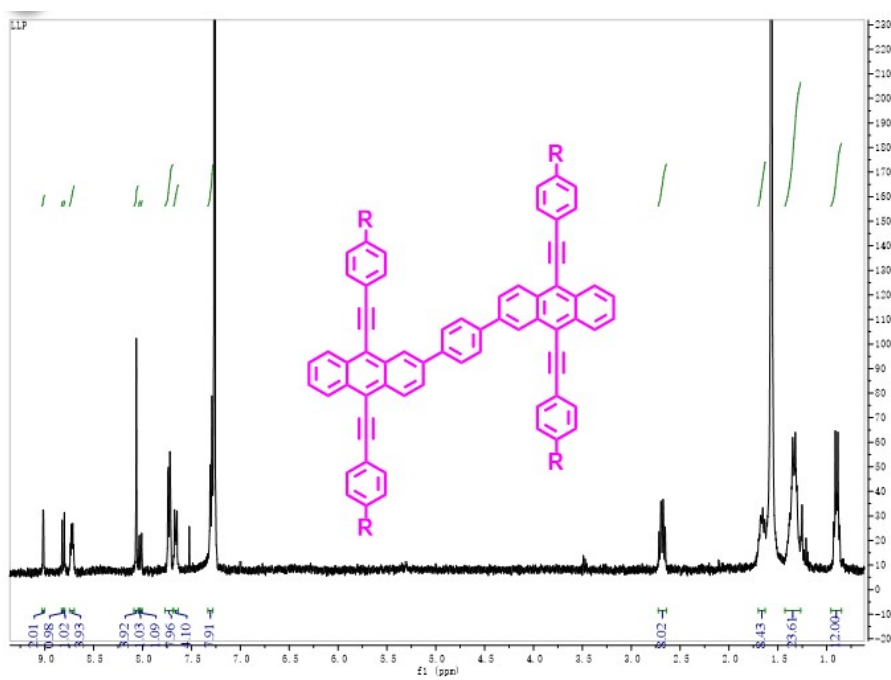


Fig. S4 The ^1H NMR spectrum of *p*-dimer.

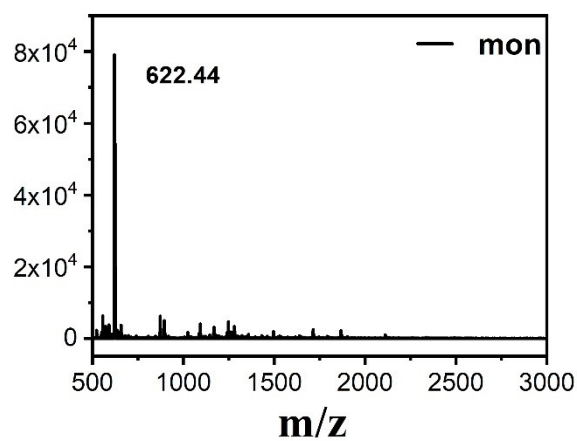


Fig. S5 The MALDI-TOF spectrum of Ph-BPEA

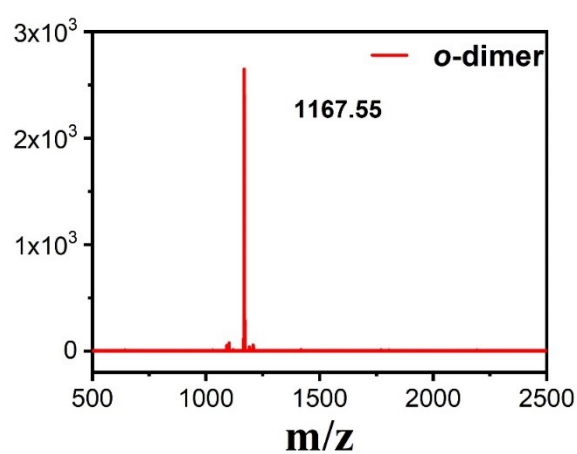


Fig. S6 The MALDI-TOF spectrum of *o*-dimer.

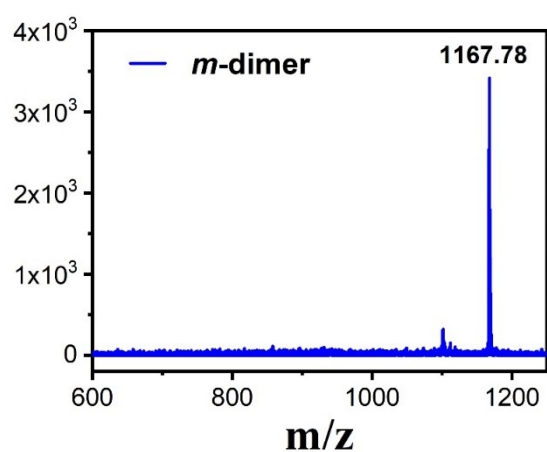


Fig. S7 The MALDI-TOF spectrum of *m*-dimer.

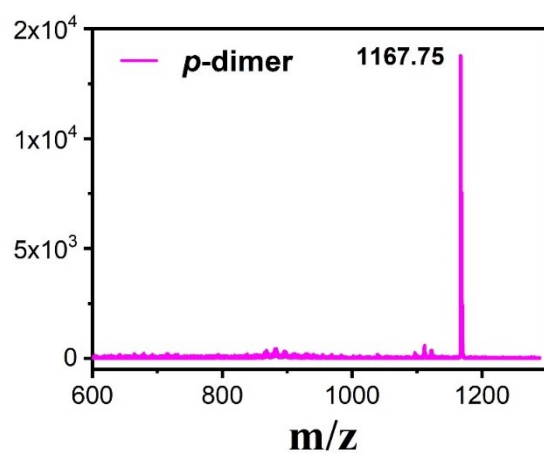


Fig. S8 The MALDI-TOF spectrum of *p*-dimer.

2. CV and DPV of Ph-BPEA and *o*-/*m*-/*p*- dimer

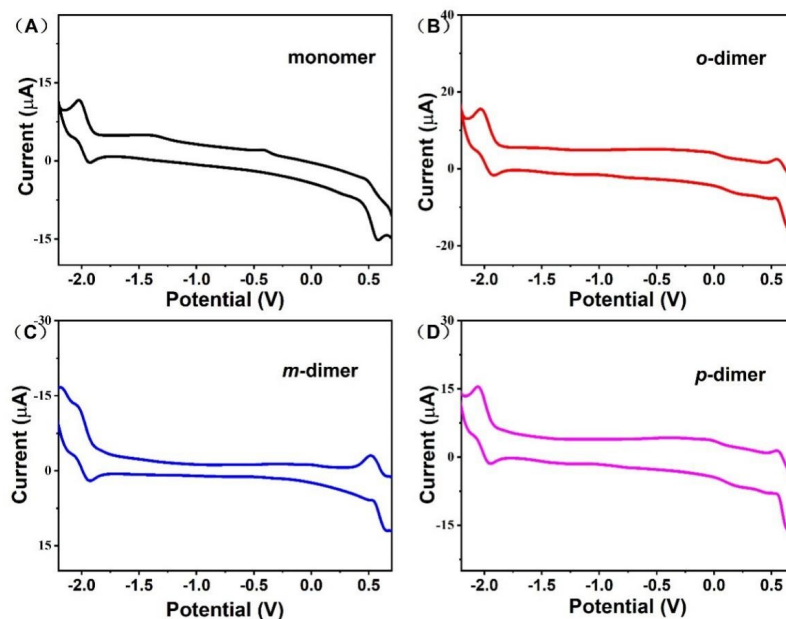


Fig. S9 CV plots of *o*-dimer, *m*-dimer and *p*-dimer as well as their monomer in dry dichloromethane containing 0.1 M (nBu)₄NPF₆ as the supporting electrolyte and ferrocene as an internal reference.

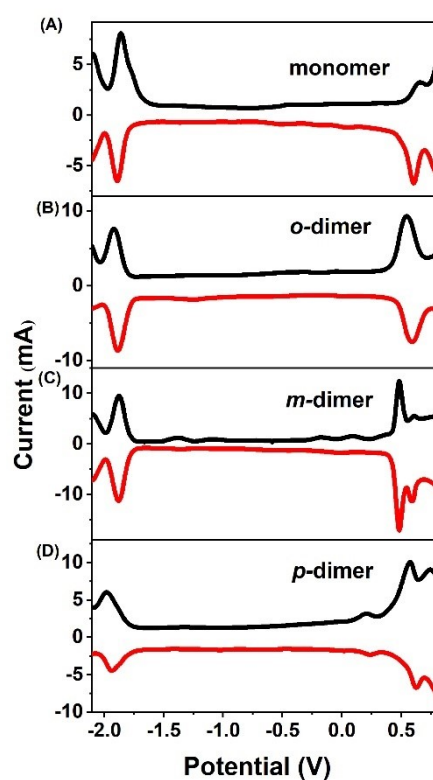


Fig. S10 DPV plots of *o*-dimer, *m*-dimer and *p*-dimer as well as their monomer in dry dichloromethane containing 0.1 M (nBu)₄NPF₆ as the supporting electrolyte and ferrocene as an internal reference.

3. Solvent-polarity-dependent absorption experiment of *o*-/*m*-/*p*- dimer

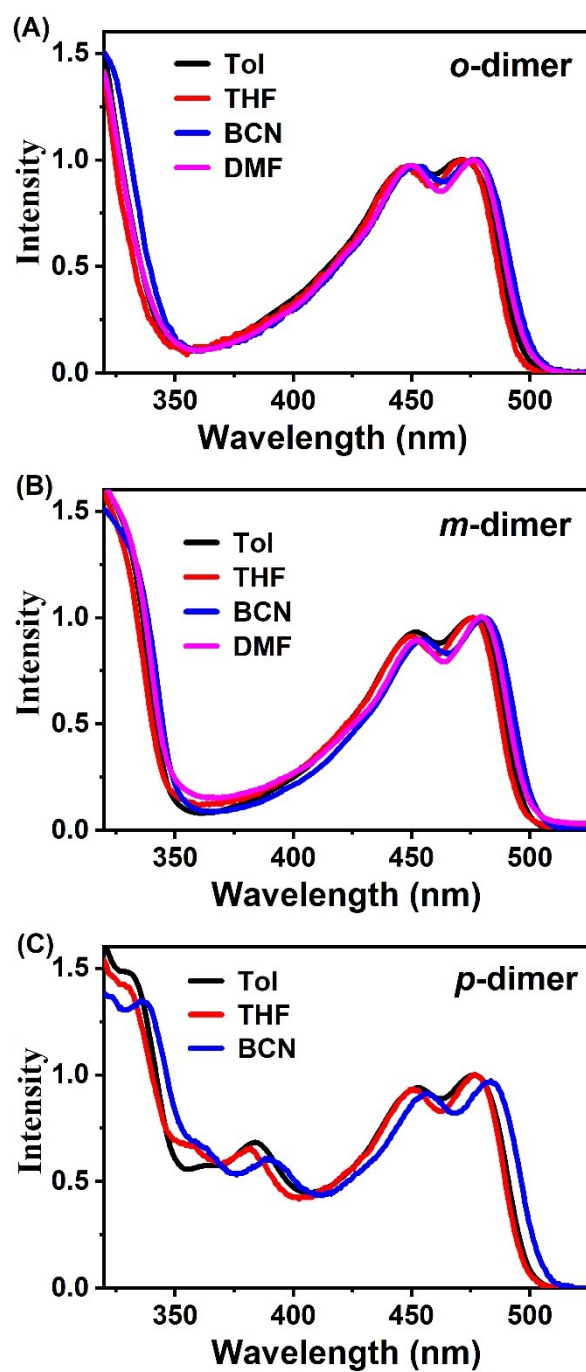


Fig. S11 Absorption spectra of *o*-dimer (A), *m*-dimer (B) and *p*-dimer (C) in different polarity solvents.

4. The fluorescence spectra and dynamics of monomer Ph-BPEA

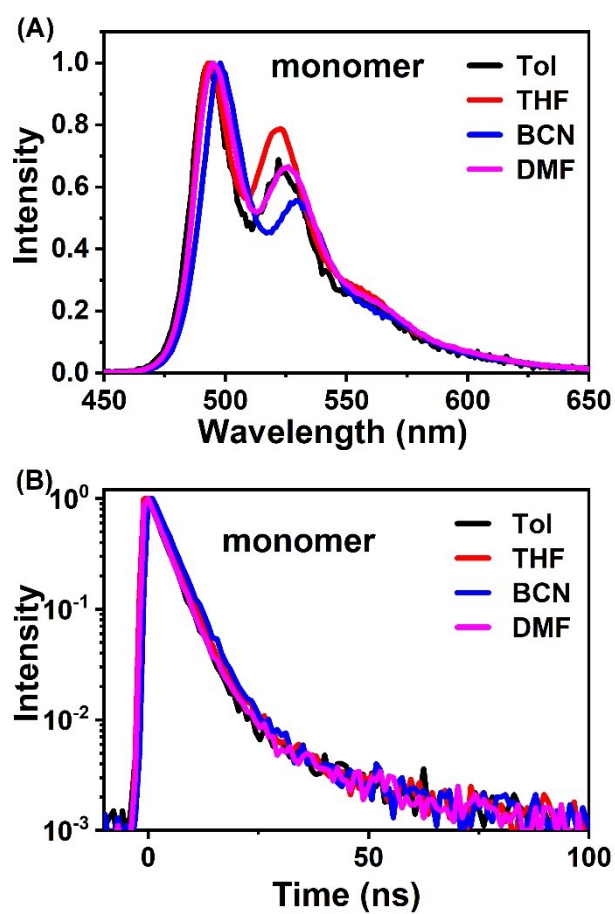


Fig. S12 The fluorescence spectra (A) and dynamics (B) of monomer Ph-BPEA.

5. *fs*-TA spectra of *o*-/*m*-/*p*-dimer in THF excited at 420 nm

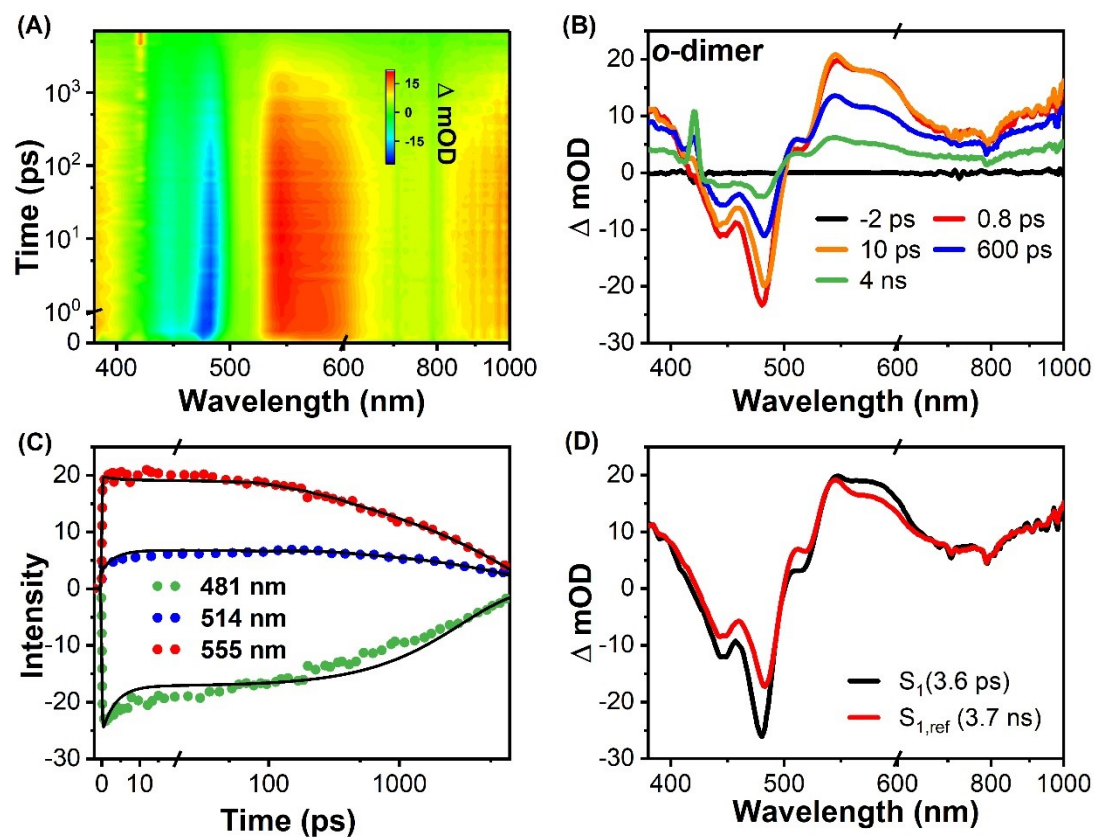


Fig. S13 (A, B) *fs*-TA spectra of *o*-dimer in THF excited at 420 nm. (C) Single-wavelength dynamics probed at different wavelengths (dotted line). The black solid line shows the fitting line from global analysis. (D) Species-associated spectra obtained from global analysis.

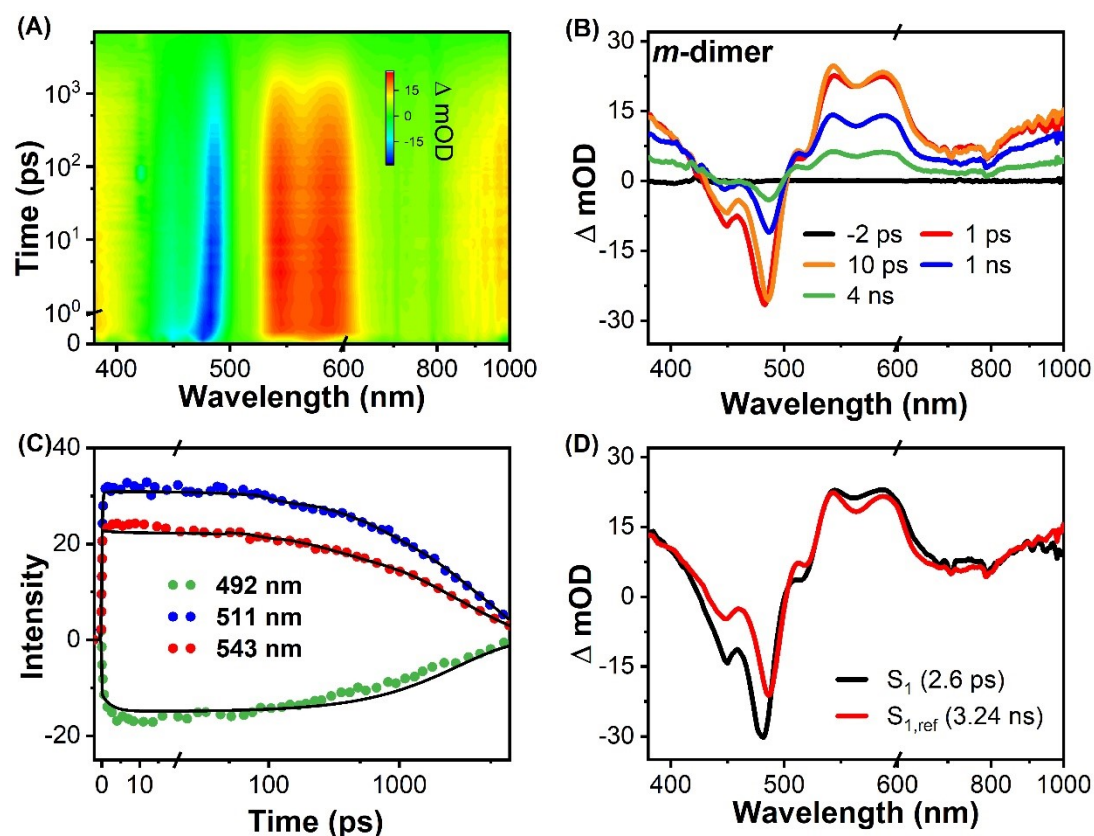


Fig. S14 (A, B) *fs*-TA spectra of *m*-dimer in THF excited at 420 nm. (C) Single-wavelength dynamics probed at different wavelengths (dotted line). The black solid line shows the fitting line from global analysis. (D) Species-associated spectra obtained from global analysis.

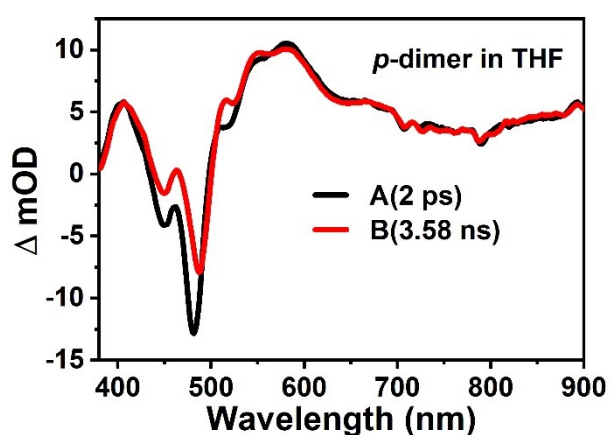


Fig. S15 Species-associated spectra of *p*-dimer in THF obtained from global analysis.

6. Electron transfer experiment

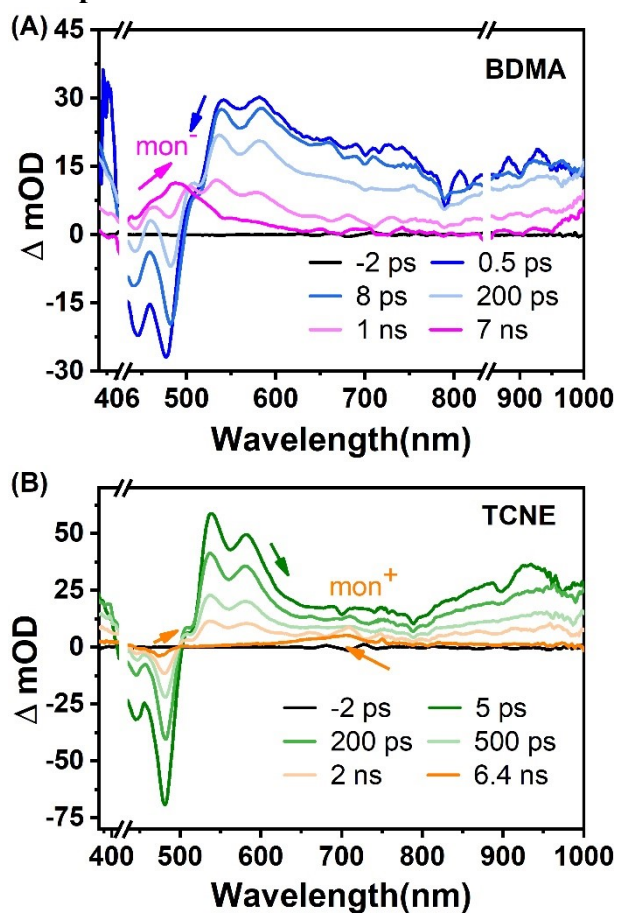


Fig. S16 *fs*-TA Spectra of monomer in the presence of N, N-dimethylphenylamine (A) or tetrachyanethene (B) excited at 420 nm.

The TA spectra of monomer Ph-BPEA in the presence of N, N-dimethylphenylamine or tetrachyanethene clearly reveal that both radical anionic and cationic features of BPEA.

7. *fs*-TA spectra of *o*-/*m*-/*p*- dimer in polystyrene (PS) film and polymethyl methacrylate (PMMA) film

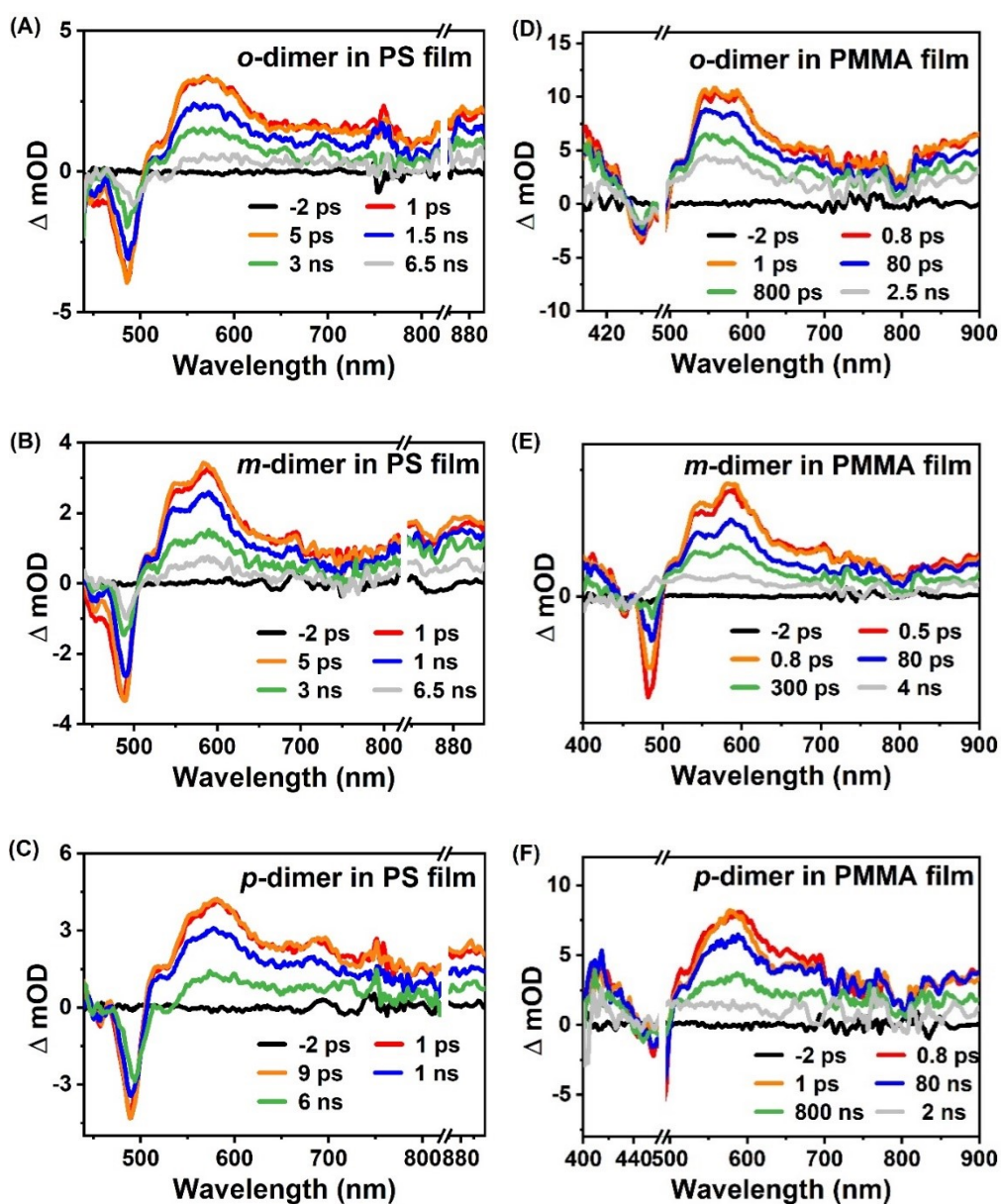


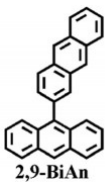
Fig. S17 *fs*-TA experiment of *o*-dimer (A, D), *m*-dimer (B, E) and *p*-dimer (C, F) in PS and PMMA film excited at 420 nm.

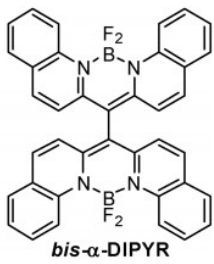
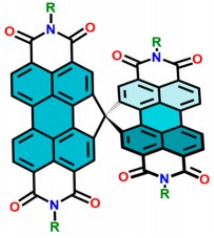
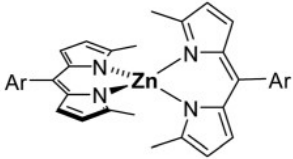
8. Charge separation and charge recombination rates

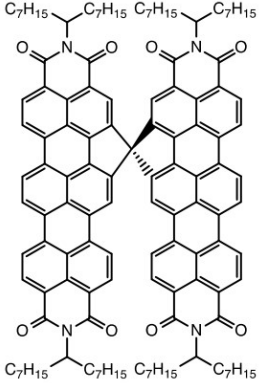
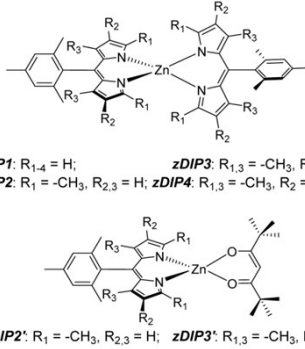
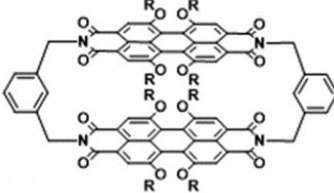
Table S1: Comparison of charge separation and charge recombination rates of *o*-/*m*-/*p*-dimer.

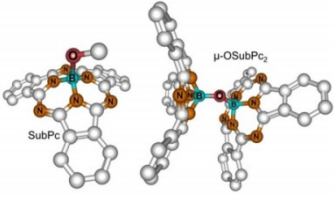
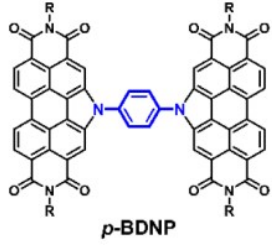
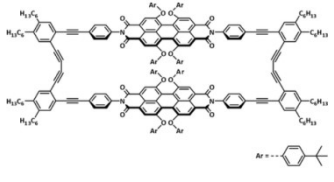
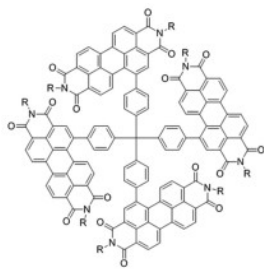
	Solvent	1/ K_{CS}	1/ K_{CR}	K_{CR}/K_{CS}
<i>o</i> -dimer	BCN	39 ps	10.3 ns	26
	DMF	8 ps	20 ns	2500
<i>m</i> -dimer	BCN	165 ps	7.1 ns	43
	DMF	77 ps	12.8 ns	166
<i>p</i> -dimer	BCN	55 ps	8.1 ns	147

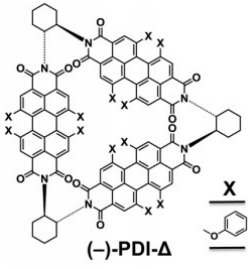
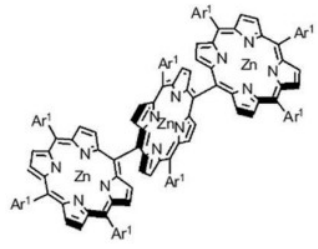
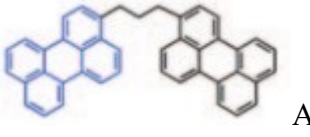
Table S2: Comparison of charge separation and charge recombination rates in different derivatives in the literature.

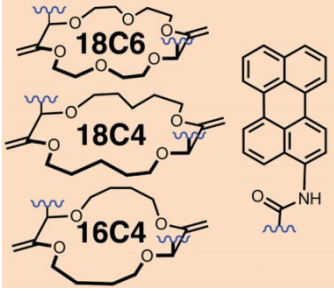
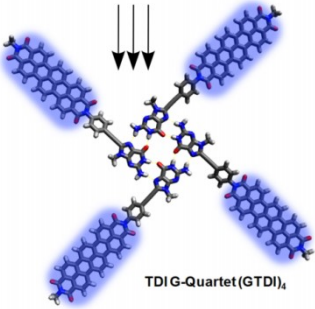
Contributed by	Molecule	Solvent	1/ K_C _S	1/ K_C _R	K_{CR}/K_{CS}
Heyuan Liu, Xiyu Li and co-workers	Orthogonal anthracene dimer  2,9-BiAn Mater. Horiz., 2019,6, 990	DMF	3.2 ps	11.6 9 ns	3653
Mark E. Thompson and co-workers	Boron dipyrindylmethene dimer	ACN	1.4 ps	4.2 ns	3000

	 <p style="text-align: center;">bis-α-DIPYR</p> <p style="text-align: center;">ACS Appl. Energy Mater. 2018, 1, 1083–1095</p>				
Ebin Sebastian and Mahesh Hariharan	<p style="text-align: center;">Spiro-conjugated perylene-3,9,10,12-tetracarboxylic diimide dimer</p>  <p style="text-align: center;">J. Am. Chem. Soc. 2021, 143, 13769–13781</p>	ACN	0.62 7 ps	1.66 ns	2647
Mark E. Thompson and co-workers	<p style="text-align: center;">two dipyrin ligands coordinated in a tetrahedral geometry at the Zn²⁺ ion</p>  <p style="text-align: center;">Faraday Discuss., 2019, 216, 379</p>	ACN	1.1 ps	0.9 ns	818
Michael R. Wasielewski and co-workers	<p style="text-align: center;">Spiro-Fused Terrylene-3,3',9,9'-tetracarboxylic diimide Dimer</p>	THF	5.9 ps	2.05 ns	339

	 <p>J. Phys. Chem. B 2021, 125, 6945–6954</p>				
Mark E. Thompson and co-workers	<p>Zinc Dipyrins</p>  <p><i>zDIP1</i>: R_{1,4} = H; <i>zDIP3</i>: R_{1,3} = -CH₃, R₂ = H; <i>zDIP2</i>: R₁ = -CH₃, R_{2,3} = H; <i>zDIP4</i>: R_{1,3} = -CH₃, R₂ = H; <i>zDIP2'</i>: R₁ = -CH₃, R_{2,3} = H; <i>zDIP3'</i>: R_{1,3} = -CH₃, R₂ = H</p> <p>J. Phys. Chem. C 2014, 118, 21834–21845</p>	polar solvents	1-5.5 ps	0.9-3.3 ns	163-333
Michael R. Wasielewski and co-workers	<p>Perylene diimide Cyclophanes</p>  <p>J. Phys. Chem. C 2020, 124, 10408–10419</p>	CH ₂ Cl ₂	23.5 ps	7.36 ns	313
Stephen R. Meech and co-workers	<p>Subphthalocyanine Dimer</p>	ACN	1.2 ps	307 ps	255

	 <p>Angew. Chem. Int. Ed. 2021, 60, 10568 – 10572</p>				
Andong Xia and co-workers	<p>Isomeric N-Annulated Perylene Diimide Dimers</p>  <p><i>p</i>-BDNP</p> <p>J. Am. Chem. Soc. 2019, 141, 12789–12796</p>	THF	12.4 ps	1.94 ns	156
Dongho Kim and co-workers	<p>1,6,7,12-tetra(4-tert-butylphenoxy)perylene dimer</p>  <p>J. Phys. Chem. Lett. 2019, 10, 8, 1919-1927</p>	BCN	23-25 ps	2.5-2.8 ns	121-100
Andong Xia and co-workers	<p>Multibranch Perylene Diimide Molecules</p> 	DMF	44.7 ps	4.8 ns	107

	J. Phys. Chem. Lett. 2020, 11, 10329–10339				
Michael R. Wasielewski and co-workers	<p>Perylenediimide Molecular Triangles</p>  <p>J. Am. Chem. Soc., 2015, 137,13236</p>	CH ₂ Cl ₂	12 ps	1.12 ns	93
Dongho Kim and co-workers	<p>push–pull porphyrin arrays</p>  <p>Phys. Chem. Chem. Phys., 2017, 19, 13970</p>	BCN	39 ps	760 ps	19.48
Eric Vauthey and co-workers	<p>1,3-bis(3- perylene)propane bichromophoric dyad</p>  <p>Angew. Chem. Int. Ed. 2011, 50, 7596–7598</p>	ACN	12 ps	130 ps	10.8
Eric Vauthey and co-workers	<p>perylene bichromophores</p>	18C4 ACN	4.3 ns	41.1 ns	9.5

	 <p>Chem. Sci., 2019, 10, 10629</p>	<p>18C6 ACN</p>	<p>25 ns</p>	<p>40 ns</p>	<p>1.6</p>
<p>Michael R. Wasielewski and co-workers</p>	<p>Terrylenediimide Guanine-Quadruplex</p>  <p>J. Am. Chem. Soc. 2019, 141, 17512–17516</p>	<p>THF</p>	<p>192 ps</p>	<p>1.6 ns</p>	<p>8.3</p>

9. Theoretical calculation

The Gibbs free energy are calculated based on the Rehm–Weller equation¹⁻³.

$$\Delta G_{CS} = e(E_{OX} - E_{RED}) - E^* + \Delta G_S \quad (1)$$

$$\Delta G_S = -\frac{e^2}{4\pi\epsilon_0\epsilon_S R_{CC}} - \frac{e^2}{8\pi\epsilon_0} \left(\frac{1}{R_A} + \frac{1}{R_D} \right) \left(\frac{1}{\epsilon_{REF}} - \frac{1}{\epsilon_S} \right) \quad (2)$$

$$\Delta G_{CR} = (-E^* + \Delta G_{CS}) \quad (3)^4$$

Where, E_{OX} and E_{RED} are the first oxidation and first reduction potentials of *o/m/p*-dimer in CH_2Cl_2 calculated by cyclic voltammetry (CV) and differential pulse voltammetry (DPV) with the ferrocene/ferrocenium (Fc/Fc^+) couples as reference. (Fig. S9, S10). ϵ_S is the dielectric constant of the actual solvent (Tol, THF, BCN and DMF, with $\epsilon = 2.38, 7.58, 24.50$ and 36.70 , respectively). E^* is the energy of the singlet excited state. ϵ_{REF} is the dielectric constant of the reference solvent used in electrochemistry (DCM: 9.3). R_{CC} is the donor-acceptor distance. R_A and R_D are hard-sphere radii, approximately $\frac{R_{CC}}{2}$. The calculated results are shown in Table 3 of main text.

Reference

1. E. Sebastian and M. Hariharan, *ACS Energy Letter.*, 2022, **7**, 696-711.
2. R. A. Marcus, *J. Chem. Phys.*, 2020, **153**, 210401.
3. R. A. Marcus, *J. Chem. Phys.*, 1965, **43**, 679-701.
4. E. Sebastian and M. Hariharan, *J. Am. Chem. Soc.*, 2021, **143**, 13769-13781.